DOI: 10.1002/ejic.201100385

Synthesis, Structural Characterization, and Magnetic Properties of the Heteroleptic Dinuclear Nickel Selenite Complex [{Ni(TMEDA)SeO_3}$_2$]

Massimiliano Delferro,*[a] Claudia Graiff,[b] Luciano Marchiò,[b] Lisa Elviri,[b] Marcello Mazzani,[c] Mauro Riccò,[c] and Giovanni Predieri*[b]

Keywords: Nickel / Selenium / Density functional calculations / Magnetic properties

The reaction of $Ni(NO_3)_2 \cdot 6H_2O$ with Na_2SeO_3 in the presence of tetramethylethylenediamine (TMEDA) in a water/ethanol mixture yielded the heteroleptic complex [{Ni(TMEDA)SeO_3}$_2$] (**1**). Single-crystal X-ray diffraction analysis showed that complex **1** consists of a dinuclear species in which the two nickel atoms are held together by two bridging selenito anions. The crystal packing of **1** is determined by networks of hydrogen bonds, involving cocrystallized water molecules and the oxygen atoms of the bridging SeO_3^{2-} groups. The two nickel ions in **1** exhibit antiferromagnetic coupling with $J = -25.7 \pm 0.1$ cm^{-1}, in good agreement with DFT calculations. In addition, when a less sterically hindered ancillary ligand, such as ethylenediamine (en), was used, the homoleptic complex [Ni(en)$_3$](SeO_3) (**2**) was obtained.

Introduction

In the last decade, interest in the structural chemistry of selenites and tellurites has grown significantly, in view of a series of interesting properties. First, they produce solid-state structures containing channels and cavities suitable to housing the selenium or tellurium electron lone pairs and form organically templated open-framework structures.[1] In fact, their electron lone pairs can often function as "chemical scissors", which break up three-dimensional networks, giving rise to layered or hollow structures.[2,3] Moreover, the presence of electron lone pairs also affords non-centrosymmetric compounds displaying useful properties such as second-order nonlinear optical (NLO) behavior,[4] ferroelectricity, and piezoelectricity.[3] In addition, the bridging properties of selenites and tellurites to connect to transition metal cations permits magnetic exchange between paramagnetic centers.[5] Finally, the weakly coordinative capability of the Se^{IV} and Te^{IV} electron lone pairs could give rise to supramolecular interactions, as observed for the polyoxoselenitepalladate anions $[Pd_{15}(\mu_3\text{-}SeO_3)_{10}(\mu_3\text{-}O)_{10}Na]^{9-}$ in the solid state.[6]

Nevertheless, relatively few studies on transition metal selenites and tellurites have been reported until now. By hydrothermal synthetic methods, a number of compounds have been synthesized and structurally characterized, for example, $CoSeO_3$ and $CuSeO_3$,[7] $NiSeO_3$ and $MnSeO_3$,[8] $PdSeO_3$,[9] $MnTeO_3$, $CoTeO_3$, and $NiTeO_3$.[10] By using suitable organic ligands it is possible to obtain oligonuclear transition metal selenite or tellurite complexes, which can be considered the building blocks of the extended solid-state structures of metal selenite and tellurite. In fact, in these oligonuclear compounds the selenite and tellurite anions exhibit the same bridging behavior between metal centers, which is the structural leitmotiv of the corresponding extended solid. In this regard, Sousa-Pedrares and coworkers[11] have reported the synthesis, structural characterization, and magnetic properties of a series of heteroleptic copper selenites with N-containing chelating bidentate ligands (phenanthroline and bipyridine). These compounds show polymeric or dinuclear structures with antiferromagnetic coupling.

In this context, we have attempted the synthesis of heteroleptic selenite complexes of nickel(II) with aliphatic bidentate amines with different steric demand, such as *N*,*N*′-tetramethylethylenediamine (TMEDA) and ethylenediamine (en). The relevant results are reported in this paper, dealing in particular with the synthesis, structural characterization, and magnetic properties, along with DFT calculations, of the heteroleptic dinuclear nickel selenite complex [{Ni(TMEDA)SeO_3}$_2$] (**1**). By using the less sterically demanding ethylenediamine (en) as a chelating ligand, the homoleptic mononuclear complex [Ni(en)$_3$]SeO_3 (**2**) is obtained, in which the selenite anion does not participate in the coordination to the Ni^{2+} cation.

[a] Department of Chemistry, Northwestern University, Evanston, Illinois 60208-3113, USA
Fax: +1-847-491-7713
E-mail: m-delferro@northwestern.edu
[b] Dipartimento di Chimica Generale ed Inorganica, Chimica Analitica, Chimica Fisica Università di Parma, Viale G. P. Usberti 17/A, 43100 Parma, Italy
Fax: +39-0521-905557
E-mail: giovanni.predieri@unipr.it
[c] Dipartimento di Fisica, Università di Parma, Viale G. P. Usberti 7/A, 43100 Parma, Italy
Supporting information for this article is available on the WWW under http://dx.doi.org/10.1002/ejic.201100385.

Results and Discussion

This paper deals with the synthesis, characterization, and magnetic properties of the heteroleptic selenite Ni^{2+} complex with *N*,*N*′-tetramethylethylenediamine as ancillary ligand. In addition, the homoleptic selenite Ni^{2+} complex, with the ethylenediamine ligand, is also reported. These ancillary ligands were chosen in order to avoid the formation of polymeric solid-state inorganic structures, due to the ability of the XO_3^{2-} moiety (X = S, Se, Te)[3] to bridge metal centers and form extended structures.

Synthesis and Structural Characterization of Complexes 1 and 2

Green crystals of binuclear complex [Ni(TMEDA)-$(SeO_3)]_2 \cdot (H_2O)_8$ (**1**) were obtained by reacting an aqueous solution of Na_2SeO_3 with an ethanol solution of tetramethylethylenediamine (TMEDA) and $Ni(NO_3)_2 \cdot 6H_2O$, followed by slow evaporation of the solvents (Scheme 1). Variations of the molar ratios of Ni^{2+}/TMEDA do not afford any products other than **1**. Formation of the tris(tetramethylethylenediamine)nickel cation $[Ni(TMEDA)_3]^{2+}$ is not favorable, due to the steric hindrance of the TMEDA ancillary ligand.[12] Mass spectroscopic analysis of **1** (by ESI-MS, Figure S1), carried out in methanol solution, indicated the presence of dinuclear complex **1** even in solution, suggesting its high stability.

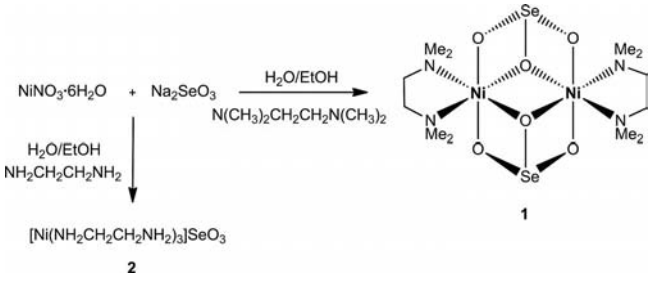

Scheme 1. Synthesis of complexes **1** and **2**.

Compound **1** crystallizes in the $P2_1/n$ space group, and the asymmetric unit is represented by the Ni(TMEDA)SeO_3 fragment that gives rise to a dinuclear structure with a center of symmetry lying between the two nickel atoms. Each metal is in a slightly distorted octahedral geometry achieved by the *N*,*N*-bidentate TMEDA ligand and by four oxygen atoms from two bridging selenite anions (Figure 1). Two of these oxygen atoms behave as oxido bridges, as they directly link the two metal centers, whereas the remaining oxygen atoms connect the two metals through the O–Se–O moiety. This behavior influences the coordination bond lengths, since the Ni–O separation involving the oxido bridge [Ni–O1 2.170(1) Å] is significantly longer than those originating from the O–Se–O bridge [Ni–O2 2.078(1) and Ni–O3 2.085(1) Å].

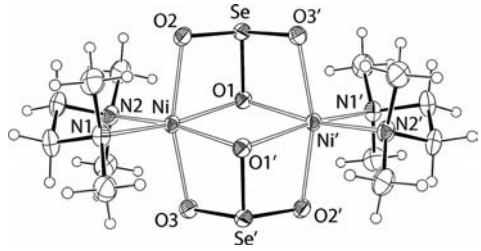

Figure 1. ORTEP drawing of **1** with thermal ellipsoids at the 30% probability level. The crystallization water molecules are omitted for clarity. Symmetry codes: ′ = 1 – *x*; 1 – *y*; 1 – *z*. Selected bond lengths [Å] and angles [°]: Ni–O1 2.169(1), Ni–O2 2.078(1), Ni–O3 2.085(1), Ni–N1 2.114(2), Ni–N2 2.121(2); N1–Ni–N2 85.47(7), O1–Ni–O2 73.27(5), O2–Ni–O3 162.12(6), O1–Ni–O3 94.50(5), O1–Ni–O1′ 80.28(5), O2–Ni–O1′ 91.84(5), O3–Ni–O1′ 72.92(5).

The Se–O bond pertaining to the oxido bridge is significantly longer than the other two Se–O bonds [Se–O1 1.727(1), Se–O2 1.687(1), Se–O3 1.686(1) Å]. The O–Se–O angles are smaller than 109°, which is in agreement with the presence of the active lone pair on the selenium atom. Nevertheless, the O(2)–Se–O(3) angle [105.68(7)°], which involves the nonbridging oxygen atoms, is significantly wider than the other two, O(2)/O(3)–Se–O(1) [96.06(6) and 95.90(6)°]. The metal–metal separation is 3.329(1) Å, which is at the upper boundary of the intermetallic separation found for dinuclear nickel systems.[13] All the oxygen atoms of the selenite anion act as hydrogen bond (HB) acceptors towards cocrystallized water molecules. In particular, the O1s water molecule exchanges a HB with O1 and O2 of a symmetry-related dinuclear complex (Figure 2).

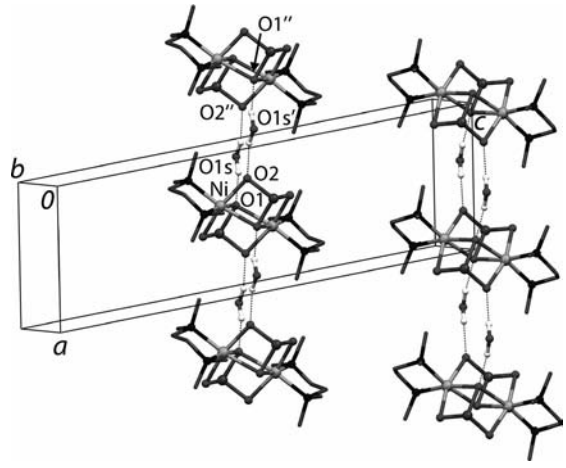

Figure 2. Portion of the crystal packing of **1** depicting the molecular chains that run parallel to the crystallographic axis *a*. The O2s, O3s, and O4s crystallized water molecules are omitted for clarity. Hydrogen bonds are shown as dashed lines. Symmetry codes: ′ = –*x*; 1 – *y*; 1 – *z*, ″ = *x* – 1; *y*, *z*. Selected hydrogen bond lengths [Å]: O1s···O1 2.780(3), O1s···O2s″ 2.778(3).

These interactions are responsible for the formation of supramolecular chains that run parallel to the crystallographic axis *a*. Overlying chains are connected by means of the O3s (HB donor) and O1s (HB acceptor), whereas paral-

lel chains facing each other with the TMEDA moiety are connected by means of an extensive net of HBs involving the O2s, O3s, and O4s water molecules (Figure 3).

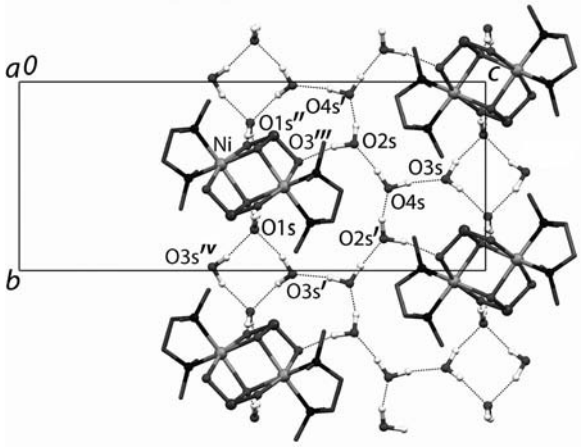

Figure 3. Portion of the crystal packing of **1** depicting the connections between the molecular chains occurring through the O2s, O3s, and O4s water molecules. Hydrogen bonds are shown as dashed lines. Symmetry codes: ′ = 1/2 – *x*; 1/2 + *y*; 3/2 – *z*, ″ = –*x*; 1 – *y*, 1 – *z*, ‴ = 1 – *x*; 1 – *y*; 2 – *z*. Selected hydrogen bond lengths [Å]: O1s···O3s′ 2.808(3), O1s···O3s′^{v} 2.824(3), O3s···O4s 2.751(3), O4s···O2s 2.761(3), O2s–O4s′ 2.753(3), O2s···O3‴ 2.829(3).

To the best of our knowledge, the coordination mode (μ_2-$\kappa^4O,O':O',O''$) of the selenito group present in complex **1** is new and in general unusual for chalcogenite anions (XO_3^{2-}, X = S, Se, Te). Only few examples are reported in the literature for this kind of coordination mode: the discrete complex [Cd(2,4,6-tri-2-pyridyl-1,3,5-triazine)-$(SO_3)]_2$,[14] and the infinite chain of the dimer [Zn(4,4′-trimethylenedipiperidine)$(SO_3)]_2$.[15]

By reacting an ethanol solution of $Ni(NO_3)_2{\cdot}6H_2O$ and ethylenediamine (en) with a water solution of Na_2SeO_3, water-soluble pink compound $[Ni(en)_3](SeO_3)$ (**2**) was obtained (Scheme 1). Variations of the molar ratios of Ni^{2+} to ancillary ligand do not afford any products other than **2**, probably due to the high stability of tris-chelate $[Ni(en)_3]^{2+}$ complex ($\log\beta_3 \approx 17.5$).[16] In addition, a small amount of insoluble $NiSeO_3$ was also formed, which was filtered off and identified by infrared spectroscopy.[5–8] Crystals of complex **2** suitable for X-ray diffraction analysis were obtained by slow concentration of the mother liquor at room temperature.

The IR spectrum of **2** exhibits the typical bands of N–H and C–H stretching above and below 3000 cm^{-1}. Characteristic N–H bending peaks are also observed at 1588 cm^{-1}. In complex **1**, the band around 640 cm^{-1} can be attributed to the SeO_3^{2-} anion,[17] hydrogen-bonded to the coordinated ethylenediamine ligand (vide infra).

Compound **2** crystallizes in the trigonal space group $P\bar{3}1c$, and its molecular structure is shown in Figure 4. The metal is in a regular octahedral geometry bound by three bidentate ethylenediamine ligands. The SeO_3^{2-} anion is located over a face of the $[Ni(en)_3]^{2+}$ octahedron, and the O1 oxygen atoms exchange hydrogen bonds with the nitrogen atoms of three ethylenediamine ligands.

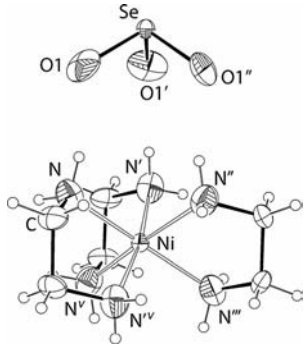

Figure 4. ORTEP drawing of **2** with thermal ellipsoids at the 30% probability level. The second selenite image was omitted for clarity. Symmetry codes: ′ = 1 – *y*; *x* – *y*; *z*, ″ = 1 – *x* + *y*; 1 – *x*; *z*; ‴ = *x*; *x* – *y*; 1/2 – *z*; ′^{v} = 1 – *x* + *y*; *y*; 1/2 – *z*; ^{v} = 1 – *y*; 1 – *x*; 1/2 – *z*. Selected bond lengths [Å]: Ni–N 2.103(8), Se–O1 1.79(2).

Magnetic Properties of Heteroleptic Complex 1

The temperature dependence of the magnetic susceptibility is identical in the FC and ZFC protocols, and it is displayed in Figure 5. The main feature is a transition from high-temperature paramagnetism to an antiferromagnetic ordered state slightly above 30 K.

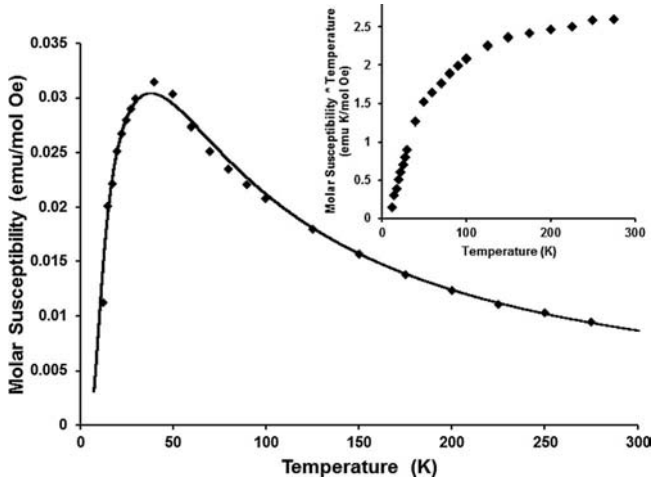

Figure 5. Temperature dependence of the magnetic susceptibility of complex **1**, measured in an applied field of 500 Oe. The solid line is the fit of Equation (1) to the experimental data (diamonds) with $J = -25.7 \pm 0.1$ cm^{-1}, $C = 1.42 \pm 0.01$ emu K mol^{-1} Oe^{-1}, and $\rho = 0$.

Some samples also showed an additional Curie contribution at low temperatures, due to small amounts of paramagnetic impurities (Figure S2).[18] Besides these temperature-dependent contributions, a minor temperature-independent part is also observed. The latter amounts to 2.7×10^{-4} emu/mol and comes from the sum of the orbital paramagnetism of nickel, which is known to be 3×10^{-4} emu/mol in selenite,[5] and a residual diamagnetic contribution. Ferromagnetic contributions from eventual impurities are absent, as confirmed by the field dependency of magnetization at room temperature. In order to evaluate the energy of the antiferromagnetic interactions, we per-

formed least-squares analysis of our data by using the model function proposed for similar nickel molecular clusters:[19]

$$\chi(T) = \rho\frac{C}{T} + (1-\rho)\frac{3C}{T}\frac{\exp\frac{J}{\kappa_B T} + 5\exp\frac{3J}{\kappa_B T}}{1 + 3\exp\frac{J}{\kappa_B T} + 5\exp\frac{3J}{\kappa_B T}} \quad (1)$$

Here ρ is the fraction of paramagnetic impurities, C the Curie constant, and J the exchange constant. Best-fit values of J vary slightly from sample to sample in the range –24.6 to –25.7 cm^{-1}.

In order to further investigate the magnetic coupling between the two metal centers in the dinuclear complex, DFT calculations were performed on the "naked" $[Ni(\mu\text{-}SeO_3)(TMEDA)]_2$ and the "hydrated" $[Ni(\mu\text{-}SeO_3)(TMEDA)]_2\cdot 6H_2O$ species. As revealed by the X-ray structure, eight water molecules are present per each dinuclear entity, and six of these interact with the six oxygen atoms of the two bridging selenite anions by means of hydrogen bonds (namely O1s, O2s and their symmetry related molecules). In addition, only one water molecule links in an intermolecular fashion to two dinuclear complexes (O1s), whereas the other water molecules are involved in an extensive net of hydrogen bonds with surrounding water molecules. It is documented that, by virtue of the hydrogen bond, the spin polarization can be transmitted intermolecularly,[20] but the weak magnetic interaction that might occur between dinuclear entities by means of the bridging O1s will not be considered in this study. We have in fact focused on the influence exerted by the water molecules that surround the first coordination sphere on the magnitude of the magnetic coupling. For this purpose, we have compared the magnetic and electronic properties of $[Ni(\mu\text{-}SeO_3)(TMEDA)]_2$ and $[Ni(\mu\text{-}SeO_3)(TMEDA)]_2\cdot 6H_2O$. The calculated J values for the "naked" (J = –32 cm^{-1}) and "hydrated" (J = –27 cm^{-1}) forms point to an antiferromagnetic coupling between the two metal centers, which is in very good agreement with the experimental findings. The coupling between the two metals occurs primarily through the bridging oxygen atom O1 and also to a minor extent through the O–Se–O bridge (Figure 6, Table 1, and Figure S3), as attested by the spin density distribution.

The "hydrated" form exhibits an absolute value of J that is slightly smaller than that of the "naked" species. This suggests that the six water molecules minimally affect the antiferromagnetic coupling between the two Ni^{2+} cations. The spin density at the metal centers for the HS (ferromagnetic quintet) and BS states (antiferromagnetic singlet) is around +1.6/+1.6 and +1.6/–1.6, respectively, confirming the localized nature of the spin at the metal centers (see Figure 6 and Figure S3). The remaining spin density is distributed on the donor atoms that constitute the coordination sphere of the Ni^{2+} centers. Moreover, the spin density localized on the metal centers has the shape of an octahedron with empty faces in agreement with the $t^6_{2g}e_g^2$ configuration of the Ni^{2+} cations. The $<S^2>$ values for the HS ferromagnetic and the BS antiferromagnetic states are in accordance with the theoretical values of 6 and 2, respectively.[21] Only one other example of a heteroleptic selenite-

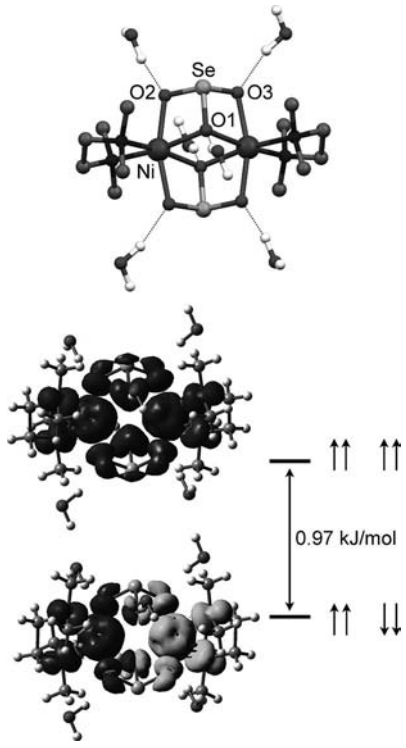

Figure 6. Energy levels of the antiferromagnetic singlet and of the ferromagnetic quintet with hydrogen-bonded water molecules of complex **1**. The total spin density is reported (B3LYP/TZVP). Dark and light gray refer to α- and β-spin density, respectively (isosurface plot at 0.001 esu $Å^{-3}$).

Table 1. Relative energies, Mulliken spin densities (ρ), Mulliken charges (q), and expectation values of the $<S^2>$ operator for the hydrated ferromagnetic quintet and for the BS antiferromagnetic singlet for $[Ni(\mu\text{-}SeO_3)(TMEDA)]_2\cdot 6H_2O$, B3LYP/TZVP.

	Ferromagnetic quintet	Antiferromagnetic singlet
Relative energy (kJ/mol)	+0.9771	0
ΔE (cm^{-1})		+81.680
Spin densities (ρ)		
Ni	+1.6660/+1.6660	+1.6634/–1.6634
O(1)	+0.0721	+0.0018/–0.0018
O(2)	+0.0425	+0.0361/–0.0361
O(3)	+0.0407	–0.0324/+0.0324
Se	+0.0283	–0.0008/+0.0008
Atomic charges (q)		
Ni	+0.738/+0.738	+0.738/+0.738
O(1)	–0.681	–0.681
O(2)	–0.638	–0.637
O(3)	–0.633	–0.632
Se	+0.895	+0.894
$<S^2>$	6.0073	2.0015

bridged dinuclear complex, [Cu(1,10-phenanthroline)-(SeO_3)]$_2$, has been described, and its magnetic properties were reported.[11] In the [Cu(1,10-phenanthroline)(SeO_3)]$_2$ complex, the SeO_3^{2-} group bridges the two Cu^{2+} ions through two oxygen atoms, while the third oxygen atom is involved in hydrogen bonding with water molecules of crystallization. The J value obtained for this compound, –22.1 cm^{-1}, is very similar to that obtained for **1**, even though the metals, the ancillary ligand, and the coordination mode of the selenito group are different.

Conclusions

This work gives further insight into the chemistry of a selenite anion and its reactivity towards a Ni^{2+} cation in the presence of ancillary ligands with different steric hindrance. In the case of the chelating ligand TMEDA, the heteroleptic dinuclear selenite complex [{Ni(TMEDA)SeO_3}$_2$] (**1**) was obtained, in which the two nickel atoms are held together by the bridging selenito groups. On the other hand, when the less sterically demanding ethylenediamine (en) was used as the chelating ligand, the mononuclear homoleptic complex [Ni(en)$_3$]SeO_3 (**2**) was formed, in which the selenite anion does not participate in the coordination to the Ni^{2+} cation. In complex **1**, the two nickel ions exhibit antiferromagnetic coupling with $J = -25.7 \pm 0.1$ cm^{-1}, in good agreement with DFT calculations. The reactions of Na_2SO_3 and Na_2TeO_3 with $Ni(NO_3)_2{\cdot}6H_2O$, in the presence of the ancillary ligand TMEDA, are currently being investigated in our laboratory.

Experimental Section

Materials and Methods: All manipulations were carried out at room temperature in air; ethylenediamine (en), tetramethylethylenediamine (TMEDA), $Ni(NO_3)_2{\cdot}6H_2O$, and Na_2SeO_3 were purchased and used as received (Aldrich). The C, H, N elemental analyses were carried out by using a Carlo Erba EA1108 microanalyzer. FTIR spectra (4000–400 cm^{-1}) were recorded with a Nicolet Nexus spectrophotometer equipped with a Smart Orbit HATR accessory (diamond). Experimental mass measurements were made with an LTQ XL (Thermo Electron Corporation) instrument equipped with an ESI interface operating in the positive ion (PI) mode; mass spectra were acquired over the scan range m/z = 200–2000 by using CH_3OH as solvent. The source introductions were carried on by a pneumatically assisted syringe (5 mL min^{-1}) flowing into a continuum flow (200 mL min^{-1}) of pure methanol from an LC pump (Finnigan Surveyor – Thermo Electron Corporation). The spray voltage was set to 4.5 kV, and the capillary temperature was 250 °C. All other instrumental parameters were automatically tuned in order to achieve the best ion transmission to the analyzer.

[Ni(TMEDA)(SeO_3)]$_2{\cdot}(H_2O)_8$ (1): A water solution (10 mL) of Na_2SeO_3 (0.173 g, 1 mmol) was added to an ethanol solution (15 mL) of TMEDA (0.150 mL, 1 mmol) and $Ni(NO_3)_2{\cdot}6H_2O$ (0.290 g, 1 mmol). The green mixture was stirred for 30 min and then filtered. Green crystals of [Ni(TMEDA)(SeO_3)]$_2{\cdot}(H_2O)_8$ (**1**) suitable for X-ray analysis were obtained by slow evaporation of the solvents (Yield 55%). $C_{12}H_{48}N_4Ni_2O_{14}Se_2$ (747.88): calcd. C 19.27, H 6.47, N 7.49; found C 19.05, H 6.45, N 7.38. ESI-MS (MeOH): m/z (%) = 604.9 (100) $[C_{12}H_{32}N_4Ni_2O_6Se_2 - H]^+$; 626.9 (68) $[C_{12}H_{32}N_4Ni_2O_6Se_2 - Na]^+$. FTIR (Diamond crystal HATR): $\tilde{\nu}$ = 3254 (s, br), 2996 (w), 2969 (w), 2931 (w), 2889 (w), 1659 (m), 1456 (ms), 678 (s), (br) cm^{-1}.

[Ni(en)$_3$](SeO_3) (2): Na_2SeO_3 (0.173 g, 1.0 mmol) dissolved in H_2O (10 mL) was added to an ethanol (15 mL) solution of ethylenediamine (0.2 mL, 3.0 mmol) and $Ni(NO_3)_2{\cdot}6H_2O$ (0.291 g, 1 mmol); a small amount of light green powder of $NiSeO_3$ precipitated while stirring (yield 7%) at room temperature. After 30 min, the reaction mixture was filtered. Pink crystals suitable for X-ray analysis of [Ni(en)$_3$](SeO_3) (**2**) were obtained by slow evaporation of solvents (yield 65%). $C_6H_{24}N_6NiO_3Se$ (365.94): calcd. C 19.69, H 6.61, N 22.95; found C 19.54, H 6.50, N 22.78. FTIR (Diamond crystal HATR): $\tilde{\nu}$ = 3325 (s), 3227 (s), 2942 (m), 2887 (m), 1588 (m), 1024 (vs), 640 (m), (br) cm^{-1}.

Computational Details: The calculations were performed on the dinuclear complex [Ni(TMEDA)(SeO_3)]$_2$ and on the hexahydrated form [Ni(TMEDA)(SeO_3)]$_2{\cdot}(H_2O)_6$ as experimentally derived from the X-ray geometry. The water molecules that interact via hydrogen bonding with the selenite anion were included in the calculation to investigate their influence on the exchange coupling constant. The calculations were performed without optimization, since small variations of the geometric parameters can lead to considerable perturbation of the metal–metal interaction. The gradient-corrected hybrid density functionals, B3LYP,[22,23] were employed with the triple-ξ valence plus polarization basis set TZVP.[24,25] All computations employed the unrestricted Kohn–Sham formalism.[26] The "broken-symmetry" approach, originally developed by Noodlemann, was used for the calculation of the electronic structure of the antiferromagnetic low-spin state (E_{BS}).[27] The spin Hamiltonian $\mathbf{H} = -J\mathbf{S}_1{\cdot}\mathbf{S}_2$ (where $\mathbf{S}_1$ and $\mathbf{S}_2$ are local spin operators) was considered for the calculation of the exchange coupling constant, J, which defines the nature of the interaction between two paramagnetic centers. The calculation of J was performed without spin projection, by the formula: $J = 2(E_{BS} - E_{HS})/S(S + 1)$, where E_{HS} is the energy of the high-spin state (quintet), and $S = S_1 + S_2$ (S_1 and S_2 are the local spins). This approach considers that the B3LYP broken symmetry (BS) wavefunction is a good approximate of the low-spin antiferromagnetic state.[28] All the calculations were performed with Gaussian 03 software.[29] Molecular orbital and spin density diagrams were generated with the GaussView program.[30]

Magnetic Susceptibility Measurements: Magnetic susceptibility measurements were performed with a Quantum Design MPMS XL5 superconducting quantum interference device (SQUID) magnetometer, capable of fields as high as 5 T. The powder samples were closed in precalibrated sample holders, whose contribution was cancelled by using the automatic background subtraction mode of the instrument.

X-ray Data Collection, Structure Solution, and Refinement: The intensity data for compounds **1** and **2** were collected at room temperature with a Bruker AXS Smart 1000[31] single-crystal diffractometer equipped with an area detector having graphite-monochromated Mo-K_α radiation (λ = 0.71073 Å). Crystallographic and experimental details of structures **1** and **2** are summarized in Table 2. The structures were solved by direct methods and refined by full-matrix least-squares procedures (based on F_o^2)[32] first with isotropic thermal parameters and then with anisotropic thermal parameters in the last cycles of refinement for all the non-hydrogen atoms. The hydrogen atoms were introduced into the geometrically calculated positions and refined as riding on the corresponding parent atoms, excepting the hydrogen atoms of the water molecules from crystallization in **1**, which were found in ΔF and refined iso-

tropically. In compound **2**, the selenite anions were found disordered in four positions that were refined with site occupancy factors of 0.25 each. In **2**, due to the poor data quality of the crystals, refinement restraints were applied to the Se–O bond lengths. CCDC-810239 and -810241 contain the supplementary crystallographic data for this paper. These data can be obtained free of charge from The Cambridge Crystallographic Data Centre via www.ccdc.cam.ac.uk/data_request/cif.

Table 2. Summary of crystallographic data for **1** and **2**.

	1	**2**
Formula	$C_{12}H_{48}N_4Ni_2O_{14}Se_2$	$C_6H_{24}N_6NiO_3Se$
FW	747.88	365.98
Crystal system	$P2_1/n$	$P\bar{3}1c$
Space group	monoclinic	trigonal
a (Å)	7.519(2)	9.090(4)
b (Å)	8.856(2)	9.090(4)
c (Å)	22.189(5)	9.901(4)
α (°)	90	90
β (°)	99.590(4)	90
γ (°	90	120
V (Å^3)	1456.8(6)	708.4(6)
Z	2	2
D_{calcd} (g cm^{-3})	1.705	1.716
F(000)	768	376
Crystal size (mm)	0.15 × 0.11 × 0.10	0.12 × 0.11 × 0.09
μ (cm^{-1})	38.52	39.46
Reflections collected	16847	20174
Reflections unique	3458	475
Reflections observed [$I > 2\sigma(I)$]	2992	412
	R_{int} = 0.0318	R_{int} = 0.0911
Parameters	186	35
R indices[a] [$I > 2\sigma(I)$]	$R1$ = 0.0248, $wR2$ = 0.0630	$R1$ = 0.0487, $wR2$ = 0.1017
R indices[a] (all data)	$R1$ = 0.0312, $wR2$ = 0.0649	$R1$ = 0.0557, $wR2$ = 0.1051

[a] $R1 = \Sigma||F_o| - |F_c||/\Sigma|F_o|$. $wR2 = \{\Sigma[w(F_o^2 - F_c^2)^2]/\Sigma[w(F_o^2)^2]\}$.

Supporting Information (see footnote on the first page of this article): ESI-MS spectrum of **1**, temperature dependence of the magnetic susceptibility for compound **1**, energy levels of the antiferromagnetic singlet and the ferromagnetic quintet for $[Ni(\mu\text{-}SeO_3)(TMEDA)]_2$.

Acknowledgments

Financial support by PRIN2008, "Molecular Clusters in Nanoscience", and Università degli Studi di Parma, Italy are gratefully acknowledged. M. D. thanks Ms J. P. McInnis for helpful discussions.

[1] a) B. Paterson, W. T. A. Harrison, *Z. Anorg. Allg. Chem.* **2007**, *633*, 158–161; b) J. Wontcheu, T. Schleid, *Z. Anorg. Allg. Chem.* **2005**, *631*, 309–315; c) T. E. Albrecht-Schmitt, P. M. Almond, R. E. Sykora, *Inorg. Chem.* **2003**, *42*, 3788–3795; d) Y. Porter, P. S. Halasyamani, *J. Solid State Chem.* **2003**, *174*, 441–449; e) P. M. Almond, S. M. Peper, E. Bakker, T. E. Albrecht-Schmitt, *J. Solid State Chem.* **2002**, *168*, 358–366; f) W. T. A. Harrison, *Acta Crystallogr., Sect. C* **2000**, *56*, E422.

[2] a) Z. Mayerova, M. Johnsson, S. Lidin, *Angew. Chem.* **2006**, *118*, 5730; *Angew. Chem. Int. Ed.* **2006**, *45*, 5602–5606; b) R. Becker, M. Johnsson, R. K. Kremer, H. H. Klauss, P. Lemmens, *J. Am. Chem. Soc.* **2006**, *128*, 15469–15475; c) R. Takagi, M. Johnsson, V. Gnezdilov, R. K. Kremer, W. Brenig, P. Lemmens, *Phys. Rev. B* **2006**, *74*, 014413–014421.

[3] J. G. Mao, H. L. Jiang, F. Kong, *Inorg. Chem.* **2008**, *47*, 8498–8510.

[4] a) P. C. Ray, *Chem. Rev.* **2010**, *110*, 5332–5365; b) K. M. Ok, E. O. Chi, P. S. Halasyamani, *Chem. Soc. Rev.* **2006**, *35*, 710–717; c) E. Cariati, M. Pizzotti, D. Roberto, F. Tessore, R. Ugo, *Coord. Chem. Rev.* **2006**, *250*, 1210–1233; d) O. R. Evans, W. Lin, *Acc. Chem. Res.* **2002**, *35–43*, 511; e) M. S. Wickleder, *Chem. Rev.* **2002**, *102*, 2011–2087; f) P. S. Halasyamani, K. R. Poeppelmeier, *Chem. Mater.* **1998**, *10*, 2753–2769; g) D. R. Kanis, M. A. Ratner, T. J. Marks, *Chem. Rev.* **1994**, *94*, 195–242.

[5] M. Miljak, R. Becker, M. Herak, M. Prester, O. Milat, M. Johnsson, H. Berger, *J. Phys. Condens. Matter* **2007**, *19*, 196203.

[6] M. Delferro, C. Graiff, L. Elviri, G. Predieri, *Dalton Trans.* **2010**, *39*, 4479–4481.

[7] K. Kohn, K. Inoue, O. Horie, S. Akimoto, *J. Solid State Chem.* **1976**, *18*, 27–37.

[8] A. Munoz, M. J. Martinez-Lope, H. Falcon, M. Garcia-Hernandez, E. Moran, *Dalton Trans.* **2006**, 4936–4943.

[9] a) J. Ling, T. E. Albrecht-Schmitt, *Inorg. Chem.* **2007**, *46*, 5686–5690; b) A. Arndt, M. S. Wickleder, *Eur. J. Inorg. Chem.* **2007**, 4335.

[10] M. Tromel, D. Schmid, *Z. Anorg. Allg. Chem.* **1972**, *387*, 230–231.

[11] A. Sousa-Pedrares, M. L. Duran, J. A. Garcia-Vazquez, J. Romero, A. Sousa, J. A. Real, *Inorg. Chem.* **2009**, *48*, 4031–4043.

[12] F. Basolo, R. K. Murmann, *J. Am. Chem. Soc.* **1952**, *74*, 5243–5246.

[13] CCDC Cambridge, Release **2010**.

[14] M. E. D. de Vivar, S. Baggio, M. T. Garland, R. Baggio, *Acta Crystallogr., Sect. C* **2006**, *62*, M195–M198.

[15] D. T. Nguyen, E. Chew, Q. C. Zhang, A. Choi, X. H. Bu, *Inorg. Chem.* **2006**, *45*, 10722–10727.

[16] a) NIST critically selected stability constants of metal complexes, Version 7; b) H. Bjerrum, G. Schwarzenbach, L. G. Sillerr, *Stability Constants of Metal-Ion Complexes, Section II: Organic Ligands*; The Chemical Society, London, **1957**.

[17] V. P. Verma, *Thermochim. Acta* **1999**, *327*, 63–102.

[18] a) D. Gatteschi, L. Bogani, A. Cornia, M. Mannini, L. Sorace, R. Sessoli, *Solid State Sci.* **2008**, *10*, 1701; b) J. Mrozinski, *Coord. Chem. Rev.* **2005**, *249*, 2534–2548; c) M. Verdaguer, *Science* **1996**, *272*, 698–699; d) D. Gatteschi, *Adv. Mater.* **1994**, *6*, 635–645; e) O. Khan, *Molecular Magnetism*, Wiley-VCH, New York, **1993**.

[19] D. Mandal, P. B. Chatterjee, R. Ganguly, E. R. T. Tiekink, R. Clerac, M. Chaudhury, *Inorg. Chem.* **2008**, *47*, 584–591.

[20] M. M. Matsushita, A. Izuoka, T. Sugawara, T. Kobayashi, N. Wada, N. Takeda, M. Ishikawa, *J. Am. Chem. Soc.* **1997**, *119*, 4369–4379.

[21] D. D. Dai, M. H. Whangbo, *J. Chem. Phys.* **2003**, *118*, 29–39.

[22] A. D. Becke, *Phys. Rev. A* **1988**, *38*, 3098–3100.

[23] A. D. Becke, *J. Chem. Phys.* **1993**, *98*, 5648–5652.

[24] A. Schafer, H. Horn, R. Ahlrichs, *J. Chem. Phys.* **1992**, *97*, 2571–2577.

[25] A. Schafer, C. Huber, R. Ahlrichs, *J. Chem. Phys.* **1994**, *100*, 5829–5835.

[26] R. G. Parr, W. Yang, *Density-Functional Theory of Atoms and Molecules*, Oxford University Press, New York, **1989**.

[27] a) L. Noodleman, C. Y. Peng, D. A. Case, J. M. Mouesca, *Coord. Chem. Rev.* **1995**, *144*, 199–244; b) L. Noodleman, D. A. Case, *Adv. Inorg. Chem.* **1992**, *38*, 423–470; c) L. Noodleman, *J. Chem. Phys.* **1981**, *74*, 5737–5743.

[28] a) F. Neese, *Coord. Chem. Rev.* **2009**, *253*, 526–563; b) E. Ruiz, J. Cano, S. Alvarez, V. Polo, *J. Chem. Phys.* **2006**, *124*, 107102; c) E. Ruiz, S. Alvarez, J. Cano, V. Polo, *J. Chem. Phys.* **2005**, *123*, 164110; d) E. Ruiz, J. Cano, S. Alvarez, P. Alemany, *J.*

Comput. Chem. **1999**, *20*, 1391–1400; e) E. Ruiz, P. Alemany, S. Alvarez, J. Cano, *J. Am. Chem. Soc.* **1997**, *119*, 1297–1303.

[29] M. J. Frisch, G. W. Trucks, H. B. Schlegel, G. E. Scuseria, M. A. Robb, J. R. Cheeseman, J. A. Montgomery Jr., T. Vreven, K. N. Kudin, J. C. Burant, J. M. Millam, S. S. Iyengar, J. Tomasi, V. Barone, B. Mennucci, M. Cossi, G. Scalmani, N. Rega, G. A. Petersson, H. Nakatsuji, M. Hada, M. Ehara, K. Toyota, R. Fukuda, J. Hasegawa, M. Ishida, T. Nakajima, Y. Honda, O. Kitao, H. Nakai, M. Klene, X. Li, J. E. Knox, H. P. Hratchian, J. B. Cross, C. Adamo, J. Jaramillo, R. Gomperts, R. E. Stratmann, O. Yazyev, A. J. Austin, R. Cammi, C. Pomelli, J. W. Ochterski, P. Y. Ayala, K. Morokuma, G. A. Voth, P. Salvador, J. J. Dannenberg, V. G. Zakrzewski, S. Dapprich, A. D. Daniels, M. C. Strain, O. Farkas, D. K. Malick, A. D. Rabuck, K. Raghavachari, J. B. Foresman, J. V. Ortiz, Q. Cui, A. G. Baboul, S. Clifford, J. Cioslowski, B. B. Stefanov, G. Liu, A. Liashenko, P. Piskorz, I. Komaromi, R. L. Martin, D. J. Fox, T. Keith, M. A. Al-Laham, C. Y. Peng, A. Nanayakkara, M. Challacombe, P. M. W. Gill, B. Johnson, W. Chen, M. W. Wong, C. Gonzalez, J. A. Pople, *Gaussian 03*, rev. C.02, Gaussian, Inc., Wallingford CT, **2004**.

[30] R. Dennington II, T. Keith, J. Millam, K. Eppinnett, W. L. Hovell, R. Gilliland, *GaussView*, Version 3.09, Semichem, Inc., Shawnee Mission, KS, **2003**.

[31] *SMART Software Users Guide*, Version 5.1, Bruker Analytical X-ray Systems, Madison, WI, **1999**; *SAINT Software User's Guide*, Version 6.0, Bruker Analytical X-ray Systems, Madison, WI, **1999**; G. M. Sheldrick, *SADABS*, Bruker Analytical X-ray Systems, Madison, WI, **1999**.

[32] G. M. Sheldrick, *SHELXL-97, Program for Crystal Structure Refinement*, University of Gottingen, Germany, **1997**.

Received: April 8, 2011
Published Online: June 22, 2011

